Accepted Manuscript

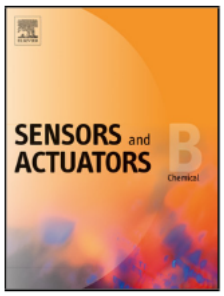

Title: Frequency Hopping Dielectrophoresis as a New Approach for Microscale Particle and Cell Enrichment

Authors: Paresa Modarres, Maryam Tabrizian

PII: S0925-4005(19)30191-1
DOI: https://doi.org/10.1016/j.snb.2019.01.157
Reference: SNB 26083

To appear in: *Sensors and Actuators B*

Received date: 27 August 2018
Revised date: 6 January 2019
Accepted date: 30 January 2019

Please cite this article as: Modarres P, Tabrizian M, Frequency Hopping Dielectrophoresis as a New Approach for Microscale Particle and Cell Enrichment, *Sensors and amp; Actuators: B. Chemical* (2019), https://doi.org/10.1016/j.snb.2019.01.157

Frequency Hopping Dielectrophoresis as a New Approach for Microscale Particle and Cell Enrichment

Paresa Modarres[1] and Maryam Tabrizian[1,2]

[1]Biomedical Engineering Department, Faculty of Medicine, McGill University, 3775 University Street, Montreal, Quebec, Canada H3A 0G4
[2]Faculty of Dentistry, McGill University, Strathcona Anatomy & Dentistry Building, 3640 University Street, Montreal, Quebec, Canada H3A 0G4

[2] Corresponding author: maryam.tabrizian@mcgill.ca

Highlights

- We introduce the concept of frequency hopping dielectrophoresis for particle sorting.
- Sorting of polystyrene microspheres with excellent purities (98.7%) was demonstrated.
- Enrichment of MCF7 cancer cells spiked in diluted blood was achieved with 82.2% efficiency.

Abstract

In the present study, we introduce a new concept termed frequency hopping dielectrophoresis (DEP) to enable a tunable microfluidic platform for microscale particle sorting. Frequency hopping DEP is used to provide a modulating force field leveraging the frequency-dependent response of polarizable particles to a non-uniform electric field. The proposed DEP platform operates by adjusting the signal parameters where a sinusoidal/square wave hops between two frequencies with a constant voltage amplitude. The two frequencies are selected such that one provides maximal DEP force (trapping frequency) and the other induces the minimal DEP force (release frequency). Analogously, the proposed DEP signaling scheme acts like the conventional microfluidic filters in which the filter size is tuned by modifying the DEP magnitude through the frequency-dependent behavior of particles. To this end, the proof-of-concept experiments were performed for the sorting of polystyrene particles of 3, 5 and 10 micrometers in diameter in a mixture with very high sorting efficiencies (98.7%). The protocol was then applied for the enrichment of MCF7 cells spiked in diluted blood samples to achieve capture efficiencies as high as 82.2%.

Keywords— Dielectrophoresis, Frequency Hopping Dielectrophoresis, Microfluidic Particle Sorting/Separation, Circulating Tumor Cell Enrichment.

1 Introduction

Sorting, purification, and enrichment of synthetic or biological particles are essential processing steps in many lab-on-a-chip platforms with broad applications in food industry, defense, and diagnostics. An application of particular interest is identification and isolation of circulating tumor cells (CTC) for diagnostics or analytical purposes. CTCs are malignant cells that have detached from the primary tumor and migrated in blood vessels. With CTCs as a fundamental prerequisite to metastasis, the enumeration of CTCs is pertinent for diagnosis, prognosis, and assessment of drug resistance [1]. Isolation of CTCs from whole blood, as the first step of the overall analysis, is a very challenging task stemming from the extremely low number of these cells, and wide heterogeneity in size, deformability, and protein expression. Despite these challenges, many techniques have been explored for CTC recognition and enrichment including immunoaffinity-based [2, 3], immunomagnetic-based [4-7], and micro-filtration [8-12]. Immunoaffinity- and immunomagnetic-based methods target membrane proteins expressed by CTCs to isolate them from blood cells. However, the major limitation of these methods is

their incapability to isolate CTCs that inherently do not express targeted proteins [13]. Using a cocktail of antibodies enhances the capture efficiency, but the process is time-consuming and cost-ineffective. Label-free techniques like micro-filtration rely on physical properties of CTCs for differentiation. Micro-filtration techniques utilize microscale features like pillars, weirs, or pores to retain desired cells based on size and deformability. However, filtration approaches are prone to clogging, and the subsequent change in flow rate increases shear stress which potentially can damage CTCs.

In recent years, dielectrophoresis (DEP), translational motion of polarized bodies in response to a non-uniform electric field, has found numerous applications in microscale and nanoscale particle handling [14, 15]. DEP techniques rely on both size and dielectric properties of cells for separation that are not addressable with other labeled- or label-free methods. Besides the cell size that significantly affects the DEP force magnitude, dielectric properties are sensitive to structural composition and morphological variations among cells providing additional criteria for differentiating CTCs from normal cells. Furthermore, DEP devices, especially those operating under AC fields, can easily be adapted for highly automated and miniaturized platforms owing to simple and inexpensive electrode fabrication and experimental setup.

DEP microfluidic platforms generally function based on the competition of hydrodynamic and DEP forces resulting in either capture/release or deflection of desired particles. For instance, Alazzam et al. implemented channel-side planar electrodes to laterally separate MDA-MB-231 breast cancer cells from blood cells achieving 81% capture efficiency [16]. However, the throughput and the lateral displacement was limited due to restrictions on channel width since the DEP force has an inverse relation with the cube of length characterizing electric-field variations ($F_{DEP} \sim V^2/L^3$). Li et al. demonstrated the separation of MDA-MB-231 cancer cells from Jurkat E6-1 T cells using an array of wireless bipolar electrodes [17]. Bipolar electrode geometry was helpful for achieving parallelization to enhance throughput; however, additional channels demanded higher voltages, up to 248 volts for a 32-channel configuration. Application of such high voltages necessitates the use of voltage amplifiers which are prohibitively expensive and bulky. Shim et al. devised a continuous flow microfluidic chamber with a slow injection of unprocessed blood that was subjected to deionization by diffusion followed by DEP exposure that was balanced out with sedimentation and hydrodynamic lift forces [18]. Equilibrium of these forces led to the transport of cancer cells to the chamber floor to be skimmed out and blood cells to an elevated height to be eluted from the channel, providing 75% sorting efficiency. This approach provides an elegant solution to process whole blood, a challenge with DEP platforms due to limitations with media conductivity. However, the deionization and levitation process require a large fluidic chamber (200 mm (L) x 25 mm (W)) and two syringe pumps, making the device fabrication and operation complicated.

Moreover, to date, most dielectrophoretic platforms are optimized based on different geometrical configurations of electrodes or exploiting various sorting strategies that mostly rely on the application of a continuous-time force field [19]. Few studies have considered tuning electrical signal parameters for realizing new modes of dielectrophoresis operation for particle sorting and manipulation. For instance, Cui et al. demonstrated size-specific elution of polystyrene particles in a mixed population using a discontinuous force field generated by a pulsed signal [20]. The pulsed signaling scheme provided a tunable mechanism for sorting a mixture containing more than two population of particles with various sizes. However, the throughput was strictly limited since the average force in time was reduced by half due to the use of a pulsed signal with 50% duty cycle. Guo et al. implemented a quadruple electrode array for moving individual cells by modulating the phase difference between electrode pairs [21].

Similarly, Zemánek et al. devised a novel microelectrode array consisting of four sectors with parallel electrodes to control movement of individual polystyrene particles within the plane of electrodes by changing the phase shift between electrodes. The phase modulation approach provided a mean for manipulating individual synthetic or biological particles in a stationary fluid. However, the applicability of this technique to particle sorting in larger scale is lacking. Furthermore, Rohani et al. applied a wave sequencing technique to induce nDEP and electrorotation (ROT) fields at different time points in order to enhance the spatial extend and frequency range for ROT characterizations [22]. Using this technique, they performed highly parallelized ROT characterization of *Cryptosporidium Parvum* after exposure to varying degrees of heat treatment. Finally, Urdaneta et al. employed a three-electrode geometry platform where two AC signals with different frequencies were applied on two electrodes while a third electrode was grounded [23]. The effective DEP force contributed from the three electrodes led to the patterning of dead and live yeast cells at separate locations between electrodes. The use of multiple frequencies at multiple electrodes was most useful for patterning different type of cells rather than dynamically sorting out a mixed population.

In the present study, we introduce a new concept termed frequency hopping DEP to enable a tunable platform for microscale particle sorting. Frequency hopping DEP is employed to provide a modulating force field leveraging frequency-dependent response of particles to a non-uniform electric field. The frequency is continuously shifted between two frequencies which induce different DEP force magnitudes on the suspending particles of various sizes and dielectric properties. By carefully choosing the frequencies and the shift rate between frequencies, particles in a multi-particle mixture can be eluted from the system according to their size and frequency-dependent signature. To this end, we present the design of a microfluidic platform to achieve sorting based on the principle of frequency hopping. For the proof of concept, separation of polystyrene microspheres based on size is presented. Very high captures efficiencies up to 99.8% were achieved for sorting a mixed population containing 3, 5, and 10 μm microspheres quantified via flow cytometry. Furthermore, the efficacy of the platform and the frequency hopping mechanism were validated by the enrichment of MCF7 cancer cells that were spiked in diluted blood samples where cancer cells were captured at electrodes, and blood cells were eluted from the channel.

The proposed frequency hopping DEP platform proved useful for sorting of synthetic particles and isolation of CTCs with the simple implementation of planer electrodes and application of small voltages (up to 20 Vpp). Moreover, the platform can easily be augmented with parallel channels for enhancing the throughput. Finally, the concept of frequency hopping DEP opens new avenues for exploring the effect of combining multiple frequencies for new DEP applications.

2 Materials and Methods

2.1 Microfluidic Platform Fabrication

The microfluidic platform consisted of gold interdigitated electrodes on the device floor with 30 μm width and 30 μm spacing, and the fluidic channel was made in SU-8 with a thickness of 30 μm, a width of 3 mm, and a length of 2.3 cm. The device fabrication involved patterning gold electrodes on a Borosilicate glass slide (SCHOTT North America, Inc., Elmsford, NY). The glass slide was first cleaned using acetone, isopropyl alcohol (IPA), and deionized water (DI) water. Next, photoresist AZ5214E was spin coated to form a 1.5 μm thick layer followed by soft baking at 110 ˚C. Then, the sample was undergone UV exposure with a dose of 20 $mJcm^{-2}$ and reversal bake at 110 ˚C for 2.5 min. Flood

exposure was followed at 450 $mJcm^{-2}$ and developing was done in MIF720 developer for 30 sec. Following the photolithography, 20 nm of Ti and 80 nm of gold was deposited using e-beam evaporation. The electrode fabrication was completed by sonication in Microposit Remover 1165 at 70 ˚C for 30 min.

Next, the glass substrate was cleaned with acetone, IPA, and rinsed with DI water followed by one-hour dehydration bake at 150 ˚C in a vacuum oven. The fluidic channel was then formed by patterning a 30 μm thick SU-8 2015 layer. First, SU-8 2015 was spin coated and soft baked at 67 ˚C and 97 ˚C for 5 and 10 min, respectively. The substrate was then UV exposed at 100 $mJcm^{-2}$ and baked at 67 ˚C for 2 min and 97 ˚C for 5 min. The sample was developed for 75 sec in the SU-8 developer to form the fluidic channel and hard baked at 150 ˚C for 10 min to relieve surface cracks and to further harden the SU-8 film.

Finally, the flow channel was sealed by bonding a PDMS layer with inlet/outlet vias to the SU-8 coated substrate. First, (3-Aminopropyl) triethoxysilane (APTES) was vacuum-deposited onto the substrate with the SU-8 layer for 1 hour [24]. The PDMS layer was plasma treated to activate the surface with oxygen groups. Then, the PDMS layer and the substrate were bonded. The bonding completed by heating the assembly on a hotplate at 100 ˚C for 5 hours under 20 N force.

2.2 Microsphere Sample Preparation

To mimic the bacterial and mammalian cells size, fluorescent polystyrene microspheres with nominal diameters of 3.1 μm, 5 μm, and 9.9 μm were purchased form Magsphere (Magsphere, Inc., Pasadena, CA). For ease of reading, round numbers 3, 5, and 10 μm are used as nominal diameters for the remainder of this article. All microspheres were in aqueous suspensions of 2.5% w/v. The microspheres were diluted by taking 1 μL of 3 μm, 4.6 μL of 5 μm, and 37 μL of 10 μm microspheres and re-suspending them in 5 mL of DI water resulting in approximately 10^3 particles per μL.

2.3 Cell Culture Sample Preparation

The working buffer for cell suspension was prepared by adding phosphate buffer saline (PBS) solution to DI water to bring the conductivity to 280 μScm^{-1}, measured using a conductivity meter (HI98303, Hanna Instruments, Woonsocket, RI). The osmolarity of the working buffer was adjusted with the addition of 8.5% sucrose, 0.1% dextrose, and 1% (w/v) bovine serum albumin (BSA). MCF7 cells (ATCC, Manassas, VA) were cultured in DMEM/High Glucose media, supplemented with 10% FBS and 1% antibiotics (v/v), and maintained in 5% CO_2 at 37 ˚C in 25 cm^2 culture flasks. Cells were harvested at 85% confluency using 0.05% trypsin-EDTA. The cell suspension was centrifuged for 3 min at 1500 rpm. Then, the media was replaced and washed twice with 2 ml of the working buffer.

2.4 Red Blood Cell Sample Preparation

Blood samples were collected from healthy volunteers in accordance with the guidelines of the ethical committee of the Montreal Heart Institute (Montreal, Canada). The blood withdrawn from the antecubital vein through a 19-gauge butterfly needle was collected in syringes containing acid citrate dextrose (Baxter Corporation, Mississauga, Canada) acting as an anticoagulant. The blood/acid citrate dextrose part ratio was 5 to 1. The collected blood was centrifuged at 3000 rpm for 15 min at room temperature. The plasma and the buffy coat were removed by aspiration. Then, 20 μL of sediments was washed with the working buffer and re-suspended in 2 ml of the working buffer containing MCF7 cells.

2.5 Cell Counting and Size Measurements

The number of cells in the final sample was counted using a hemocytometer, and the average cell radius was obtained from 30 cells measurements using light microscopy (TE-2000E, Nikon). The average red blood cell (RBC) and MCF7 radii were measured to be 4.57 ± 0.23 μm and 12.17 ± 2 μm, respectively.

2.6 Microsphere and Cell Separation Protocol

For the experiments with microspheres, the device was pre-washed with 0.1% solution of Tween 20, and the microsphere solution was continuously withdrawn into the device using a standard infuse/withdraw syringe pump (11 Elite Programmable Syringe Pump, Harvard Apparatus, Inc.). The device operation was monitored using an inverted microscope (TE-2000E, Nikon) to assess particle trajectories. The frequency hopping signal (output mode: high impedance) was generated by a function generator (AFG3200C, Tektronix, Inc.). For MCF7 cell enrichment experiments, the device was pre-washed with the working buffer for 5 min followed by continuous withdrawal of cell suspensions in working buffer using a standard infuse/withdraw syringe pump as mentioned above.

To quantify the sorting efficacy of polystyrene microspheres, 80 μL of mixed solution was withdrawn through the fluidic chamber and collected in a glass syringe used with the pump. The collected sample was transferred to a 1.5 ml vial while raising the volume to 500 μL. With the dilution parameters stated in section 2.2, 80 μl volume corresponds to approximately 80×10^3 microspheres. For flow cytometry (BD FACSCalibur™) measurements, the sample was transferred to a flow cytometry tube and mixed well with a vortex mixer. To identify the percentage of microsphere within the output population, side scattered cytometry (SSC) versus forward scattered cytometry (FSC) dot plots were attained and the reported numbers within each identified gate for fluorescent microbeads were used for percentage calculations. Flow cytometry data were expressed as the mean ± standard deviation (SD) of three replicates.

The enrichment efficiency of MCF7 cells was calculated by counting the number of captured cells and eluted cells and taking the ratio of captured cells to the sum of all cells by analyzing acquired videos at the outlet and consecutive images acquired from electrodes. For each experimental condition, a five-minute video (50 frames per second (fps)) was captured at the outlet while continuously withdrawing the cell solution followed by a cell-free buffer wash. Since the MCF7 cells were significantly different in size and shape from red blood cells and very low in number, they were easily distinguished from red blood cells and were counted on-chip by analysing captured images of electrodes. The capture efficiency data were reported as the mean ± standard deviation (SD) of three replicates.

3 Results and Discussions

3.1 Principle of Operation

Dielectrophoresis is the translational motion of polarized bodies in the presence of an electric field. In an electric field with intensity E, the average force exerted on a homogeneous spherical particle of radius r and electrical permittivity of ε_p in a media of electrical permittivity of ε_m is formulated as:

$$F = 2\pi\varepsilon_0\varepsilon_m r^3 Re[f_{cm}]\nabla|E^2| \quad (1)$$

$$f_{cm} = \frac{\varepsilon_p^* - \varepsilon_m^*}{\varepsilon_p^* + 2\varepsilon_m^*} \quad (2)$$

$$\varepsilon^* = \varepsilon - j\frac{\sigma}{\omega} \tag{3}$$

where ε_0 is the permittivity of free space, $Re\ [f_{cm}]$ is the real part of the Clausius-Mossotti (CM) factor, σ is the conductivity, ω is the radial frequency, and ε^* is the complex permittivity. The CM factor determines the polarity and strength of the induced dipole in a particle and thus provides a mean for understanding how a particle behaves in a non-uniform electric field. For positive values of $Re[f_{cm}]$, a polarized particle is attracted to the regions of highest electric field (or electrode edges), and for negative values of $Re[f_{cm}]$ factor, a particle is repelled from electrodes to the field minima. For polystyrene microspheres, the cross-over frequency (the frequency at which the DEP force is zero) is strongly dependent on the size of particles assuming all other parameters are constant. The size-dependent behavior of cross-over frequency for these particles directly stems from the conductivity (σ_p) relation with size revealed through the following relation [25, 26]:

$$\sigma_p = \sigma_{bulk} + 2\frac{K_s}{r} \tag{4}$$

where σ_{bulk} denotes the bulk conductivity, and K_s is the surface conductance. Eq. 4 was derived assuming the electrical double layer (EDL) is much thinner than the particle diameter. The parameters for polystyrene surface and bulk conductivity and permittivity values were obtained from published literature [25, 27, 28].

The size- and frequency-dependent behavior of particles in a non-uniform electric field were utilized to sort out a mixture of polystyrene microspheres of various sizes by manipulating the frequency of the applied voltage. To this end, two frequencies were identified for capturing and releasing particles. The capture frequency ($f_{capture}$) was selected such that all particles experienced either a maximum negative DEP (nDEP) force or a maximum positive DEP (pDEP) force. The release frequency ($f_{release}$) was chosen based on the cross-over frequency for each particle size such that the DEP force was reduced leading to release from the DEP capture zones.

Figure 1

To leverage the frequency hopping DEP for particle sorting, the proposed platform consisted of interdigitated electrodes (trap locations) to generate sinusoidally varying field intensities. Thereby, the application of capture frequency displaced all particles to the field traps above the nearest electrode digits (nDEP) or at electrode edges (pDEP). By adjusting the release frequency, the target particles were released from the DEP capture zones based on their cross-over frequency (Fig. 1a, 1b).

3.2 Electric Field Distribution Simulations

The electric field inside the channel was simulated using COMSOL 5.2 (Burlington, MA) to find the location of field minima and maxima where the DEP capture zones are. The 2-D cross-section of the device including the channel floor (glass), the fluid, and the channel top (PDMS) was modeled using the AC/DC module physics. The electric field square (E^2) versus location along the longitudinal axis of the device (x-direction) is illustrated in Fig. 2a. As seen in this figure, the field capture zones operating under nDEP and pDEP lie above each electrode digit near the ceiling (black bars) and electrode edges, respectively. The magnitude and spatial variation of E^2, one particle radius away from the channel top

Figure 2

3.3 Sorting of Polystyrene Microparticles

The theroetical calculation of CM curve using reported parameters in literature is illustrated in Fig. 1c. According to CM plot, an appropriate frequency to capture all polystyrene particles found to be 1 MHz. The release frequency was experimentally identified by lowering frequency to near cross-over frequency for the target particles which fell within 20 – 100 kHz range for 3 µm and 5 µm diameter microspheres.

To experimentally identify and optimize the parameters for microparticle sorting protocol in a mixed population, first, each microsphere size was withdrawn into the device at the maximum flow rate at which the nDEP force traps all incoming microspheres. The capture frequency for a maximum nDEP force was set at 1 MHz for all microsphere sizes (Fig. 1c). To find the release frequency, the frequency was lowered from 1 MHz in 1 kHz steps until microspheres started eluting from the channel. This experiment was repeated with several flow rates to have a plot of flow rate vs. threshold release frequency (Fig. 2d). Fig. 2d illustrates the threshold frequency at which particles start escaping the DEP traps for certain flow rates. As the flow rate decreases, the release frequency reduces approaching the cross-over frequency. Based on these experiments, a volumetric flow rate of 40 µL/hr was chosen to retain all microspheres. To sort a mixed population, the electrical signal and flow rate parameters were initially set to these values to capture all incoming microspheres followed by varying the release frequency for reducing the nDEP force to elute microspheres of different diameters.

The sorting efficiency of the platform was determined by analyzing the size distribution of collected microparticles before and after the voltage application using flow cytometry. For a mixed population of 3 µm, 5 µm, and 10 µm diameter microspheres, the mixed solution was withdrawn into the device in a continuous fashion at a flow rate of 40 µL/hr (ESI movie †). The composition and the percentages of microspheres in a mixed solution is shown in Fig. 4a and Fig 4d, respectively. Initially, all microspheres were trapped by applying a 20 V_{pp} sinusoidal signal ($f_{capture}$ = 1 MHz, $f_{release}$ = 1 MHz, f_{rate} = 1 Hz). To elute 3 µm microspheres and capture 5 µm and 10 µm particles, the release frequency was set at 85 kHz. As seen in Fig. 4b and Fig. 4e, 3 µm microspheres (red color) consisted 99.7% percent of retrieved microspheres at the output. To elute 3 µm and 5 µm microspheres with 10 µm microspheres trapped, the release frequency was further lowered to 20 kHz. The result of this elution is illustrated in Fig. 4c and 4f where 98.7% of collected microsphere were 3 µm and 5 µm (green color) beads with 1.3% of 10 µm beads (blue color).

Figure 3

During the sorting experiments, particle pearl-chaining was observed as the number of captured particles increased. Pearl-chaining of polarized particles happens due to electrostatic interactions between particles as a mean to reduce their electrical potential energy [29]. While the dielectrophoretic behavior of these chain-like particles is different from single microspheres [30], we noted that doublet and triplet microspheres were also released along with single microspheres of the same size. Thus, the formation of pearl-chain microspheres did not prohibit elution of these assembled particles from the channel. However, attachment of the smaller sized microspheres to the larger ones, which formed dissimilar pearl-chain assemblies, prevented the smaller sized particles to be removed from the channel when intended unless they were dissociated from the larger particles by interrupting the voltage.

Moreover, the electrodes at the beginning of the stream collected all incoming particles which led to the saturation of these electrodes, the capture of unwanted microparticles, and exacerbation of pearl-chain formation. To relieve these issues, it was necessary to disrupt the electric field by turning off the voltage in intervals to avoid the saturation problem and to allow the grouped particles to dissociate and move down the channel.

Figure 4

3.4 Enrichment of MCF7 Cells as a Model for CTCs

To test the feasibility of frequency hopping DEP for the cell enrichment, label-free capturing of MCF7 cells (a breast cancer cell line used as a model for CTC) was performed with MCF7 cells spiked in diluted blood, approximately 1 MCF7 cell for every 500 RBCs. Both MCF7 and RBCs showed a strong pDEP response collecting these cells at electrode edges for approximate frequency ranges of 350 kHz - 20 MHz and 200 kHz - 14 MHz, respectively. At frequencies below 200 kHz, a weak nDEP force was observed for both cell types. The $Re(f_{cm})$ versus frequency plot based on dielectric parameters reported in literature for MCF7 and RBCs is illustrated in Fig. 5a. The experimental observation of frequencies corresponding to pDEP and nDEP forces for MCF7 cells and RBCs were slightly different from that of predicated by the theoretical calculations. This can be explained considering the variations in cell dielectric parameters reported in the literature and the cells used in experiments as well as the simplifications that were assumed in deriving the theoretical cell models and DEP force.

To isolate MCF7 cells, the cell suspension was continuously withdrawn into the channel at 80 μL/hr with 1 MHz capture frequency and 150 kHz release frequency. With these flow and signal parameters, the MCF7 cells were captured at electrodes by pDEP force, and RBCs were eluted from the channel experiencing a weak nDEP force. The enrichment efficiency was calculated by counting the number of captured cells and eluted cells and taking the ratio of captured cells to the sum of all cells by analyzing acquired videos at the outlet and consecutive images acquired from electrodes (Fig. 5b). An enrichment efficiency as high as 82.2% was obtained for a 20 V_{pp} sinusoidal signal. At lower voltages, the sorting performance remained relatively similar down to 16 $V_{pp,}$ below which the trapping efficiency was appreciably reduced. The trapping efficiency of MCF7 cells was largely affected by inhomogeneities in shape, size, and structure of cancer cells which explain the lower capture rate of CTCs compared to that of polystyrene microparticles. For instance, individual and cluster cells with sizes considerably deviate from the average cell size were not effectively trapped. Such problems can be compensated for by designing channels with larger depth and increasing the voltage amplitude.

Figure 5

4 Conclusion

In this article, we demonstrated the efficacy of frequency hopping DEP for the sorting of polystyrene microspheres with excellent purities as high as 98.7%. The applicability of the proposed DEP platform to enrich CTC-like cells was also achieved with a separation efficiency of 82.2%, comparable to that reported in DEP-based devices so far [16, 18]. Our results convey that the concept of frequency hopping DEP is effective for sorting of particles based on variations in size only or a combination of size- and

frequency-dependent response of particles to an electric field. Additionally, in the present study, we employed a signaling scheme where frequency shifted with a 50% duty cycle. Further experiments are required to study the effect of duty-cycle on capture efficiency. Finally, frequency hopping provides a tunable platform by which multiple parameters can be altered to accomplish separation based on the size and inherent dielectric properties of cells of interest. Once a certain electrode and fluidic channel geometry is adapted, the presented DEP scheme can be leveraged for sorting of other micron-sized particles.

5 Acknowledgments

The authors gratefully acknowledge the financial support from Natural Sciences and Engineering Research Council of Canada (NSERC) through CREATE training programs in ISS (Integrated Sensors and Systems) and CFS (Continuous Flow Systems), and CGS doctoral fellowship. Additionally, the authors acknowledge kind support of colleagues, Nickolas Distasio, Kaushar Jahan and Saadia Shoaib, for assisting with flow cytometry and cell culture experiments.

References

[1] M. Cristofanilli, Circulating tumor cells, disease progression, and survival in metastatic breast cancer, Semin Oncol, 33(2006) S9-S14.

[2] S. Nagrath, L.V. Sequist, S. Maheswaran, D.W. Bell, D. Irimia, L. Ulkus, et al., Isolation of rare circulating tumour cells in cancer patients by microchip technology, Nature, 450(2007) 1235-U10.

[3] A.A. Adams, P.I. Okagbare, J. Feng, M.L. Hupert, D. Patterson, J. Gottert, et al., Highly efficient circulating tumor cell isolation from whole blood and label-free enumeration using polymer-based microfluidics with an integrated conductivity sensor, J Am Chem Soc, 130(2008) 8633-41.

[4] C.E. Yoo, J.M. Park, H.S. Moon, J.G. Joung, D.S. Son, H.J. Jeon, et al., Vertical Magnetic Separation of Circulating Tumor Cells for Somatic Genomic-Alteration Analysis in Lung Cancer Patients, Sci Rep, 6(2016) 37392.

[5] J.H. Kang, S. Krause, H. Tobin, A. Mammoto, M. Kanapathipillai, D.E. Ingber, A combined micromagnetic-microfluidic device for rapid capture and culture of rare circulating tumor cells, Lab Chip, 12(2012) 2175-81.

[6] K. Hoshino, Y.Y. Huang, N. Lane, M. Huebschman, J.W. Uhr, E.P. Frenkel, et al., Microchip-based immunomagnetic detection of circulating tumor cells, Lab on a Chip, 11(2011) 3449-57.

[7] P. Chen, Y.Y. Huang, K. Hoshino, J.X.J. Zhang, Microscale Magnetic Field Modulation for Enhanced Capture and Distribution of Rare Circulating Tumor Cells, Scientific Reports, 5(2015).

[8] K.A. Hyun, K. Kwon, H. Han, S.I. Kim, H.I. Jung, Microfluidic flow fractionation device for label-free isolation of circulating tumor cells (CTCs) from breast cancer patients, Biosens Bioelectron, 40(2013) 206-12.

[9] S.J. Tan, R.L. Lakshmi, P. Chen, W.T. Lim, L. Yobas, C.T. Lim, Versatile label free biochip for the detection of circulating tumor cells from peripheral blood in cancer patients, Biosens Bioelectron, 26(2010) 1701-5.

[10] A.F. Sarioglu, N. Aceto, N. Kojic, M.C. Donaldson, M. Zeinali, B. Hamza, et al., A microfluidic device for label-free, physical capture of circulating tumor cell clusters, Nature Methods, 12(2015) 685-+.

[11] X.Y. Fan, C.P. Jia, J. Yang, G. Li, H.J. Mao, Q.H. Jin, et al., A microfluidic chip integrated with a high-density PDMS-based microfiltration membrane for rapid isolation and detection of circulating tumor cells, Biosensors & Bioelectronics, 71(2015) 380-6.
[12] J.A. Hernandez-Castro, K. Li, A. Meunier, D. Juncker, T. Veres, Fabrication of large-area polymer microfilter membranes and their application for particle and cell enrichment, Lab on a Chip, 17(2017) 1960-9.
[13] P.K. Grover, A.G. Cummins, T.J. Price, I.C. Roberts-Thomson, J.E. Hardingham, Circulating tumour cells: the evolving concept and the inadequacy of their enrichment by EpCAM-based methodology for basic and clinical cancer research, Ann Oncol, 25(2014) 1506-16.
[14] J. Voldman, Electrical forces for microscale cell manipulation, Annu Rev Biomed Eng, 8(2006) 425-54.
[15] P. Modarres, M. Tabrizian, Alternating current dielectrophoresis of biomacromolecules: The interplay of electrokinetic effects, Sensors and Actuators B-Chemical, 252(2017) 391-408.
[16] A. Alazzam, B. Mathew, F. Alhammadi, Novel microfluidic device for the continuous separation of cancer cells using dielectrophoresis, J Sep Sci, 40(2017) 1193-200.
[17] M. Li, R.K. Anand, High-Throughput Selective Capture of Single Circulating Tumor Cells by Dielectrophoresis at a Wireless Electrode Array, Journal of the American Chemical Society, 139(2017) 8950-9.
[18] S. Shim, K. Stemke-Hale, A.M. Tsimberidou, J. Noshari, T.E. Anderson, P.R. Gascoyne, Antibody-independent isolation of circulating tumor cells by continuous-flow dielectrophoresis, Biomicrofluidics, 7(2013) 11807.
[19] K. Khoshmanesh, S. Nahavandi, S. Baratchi, A. Mitchell, K. Kalantar-zadeh, Dielectrophoretic platforms for bio-microfluidic systems, Biosens Bioelectron, 26(2011) 1800-14.
[20] H.H. Cui, J. Voldman, X.F. He, K.M. Lim, Separation of particles by pulsed dielectrophoresis, Lab Chip, 9(2009) 2306-12.
[21] X.L. Guo, R. Zhu, Controllably moving individual living cell in an array by modulating signal phase difference based on dielectrophoresis, Biosensors & Bioelectronics, 68(2015) 529-35.
[22] A. Rohani, W. Varhue, Y.-H. Su, N.S. Swami, Electrical tweezer for highly parallelized electrorotation measurements over a wide frequency bandwidth, ELECTROPHORESIS, 35(2014) 1795-802.
[23] M. Urdaneta, E. Smela, Multiple frequency dielectrophoresis, Electrophoresis, 28(2007) 3145-55.
[24] Y.F. Ren, S.H. Huang, S. Mosser, M.O. Heuschkel, A. Bertsch, P.C. Fraering, et al., A Simple and Reliable PDMS and SU-8 Irreversible Bonding Method and Its Application on a Microfluidic-MEA Device for Neuroscience Research, Micromachines, 6(2015) 1923-34.
[25] W.M. Arnold, H.P. Schwan, U. Zimmermann, Surface Conductance and Other Properties of Latex-Particles Measured by Electrorotation, J Phys Chem-Us, 91(1987) 5093-8.
[26] P.Y. Weng, I.A. Chen, C.K. Yeh, P.Y. Chen, J.Y. Juang, Size-dependent dielectrophoretic crossover frequency of spherical particles, Biomicrofluidics, 10(2016) 011909.
[27] S. Park, Y. Zhang, T.H. Wang, S. Yang, Continuous dielectrophoretic bacterial separation and concentration from physiological media of high conductivity, Lab Chip, 11(2011) 2893-900.
[28] M.D. Vahey, J. Voldman, High-Throughput Cell and Particle Characterization Using Isodielectric Separation, Analytical Chemistry, 81(2009) 2446-55.
[29] R. Pethig, Review-Where Is Dielectrophoresis (DEP) Going?, Journal of the Electrochemical Society, 164(2017) B3049-B55.
[30] B. Techaumnat, B. Eua-arporn, T. Takuma, Calculation of electric field and dielectrophoretic force on spherical particles in chain, J Appl Phys, 95(2004) 1586-93.

Figure Captions

Figure 1: Schematic illustration of device operation using frequency hopping dielectrophoresis demonstrating size-based sorting of particles in a heterogenous polystyrene population. (a) 10 μm (blue) and 5 μm (green) microspheres are retained while 3 μm (red) particles are flowing down the channel. (b) 10 μm particles are retained while 3 μm and 5 μm microspheres are released. (c) The real part of the CM factor versus frequency for polystyrene microspheres of 10 μm, 5 μm, and 3 μm diameter showing the cross-over frequency. (d) Experimental setup.

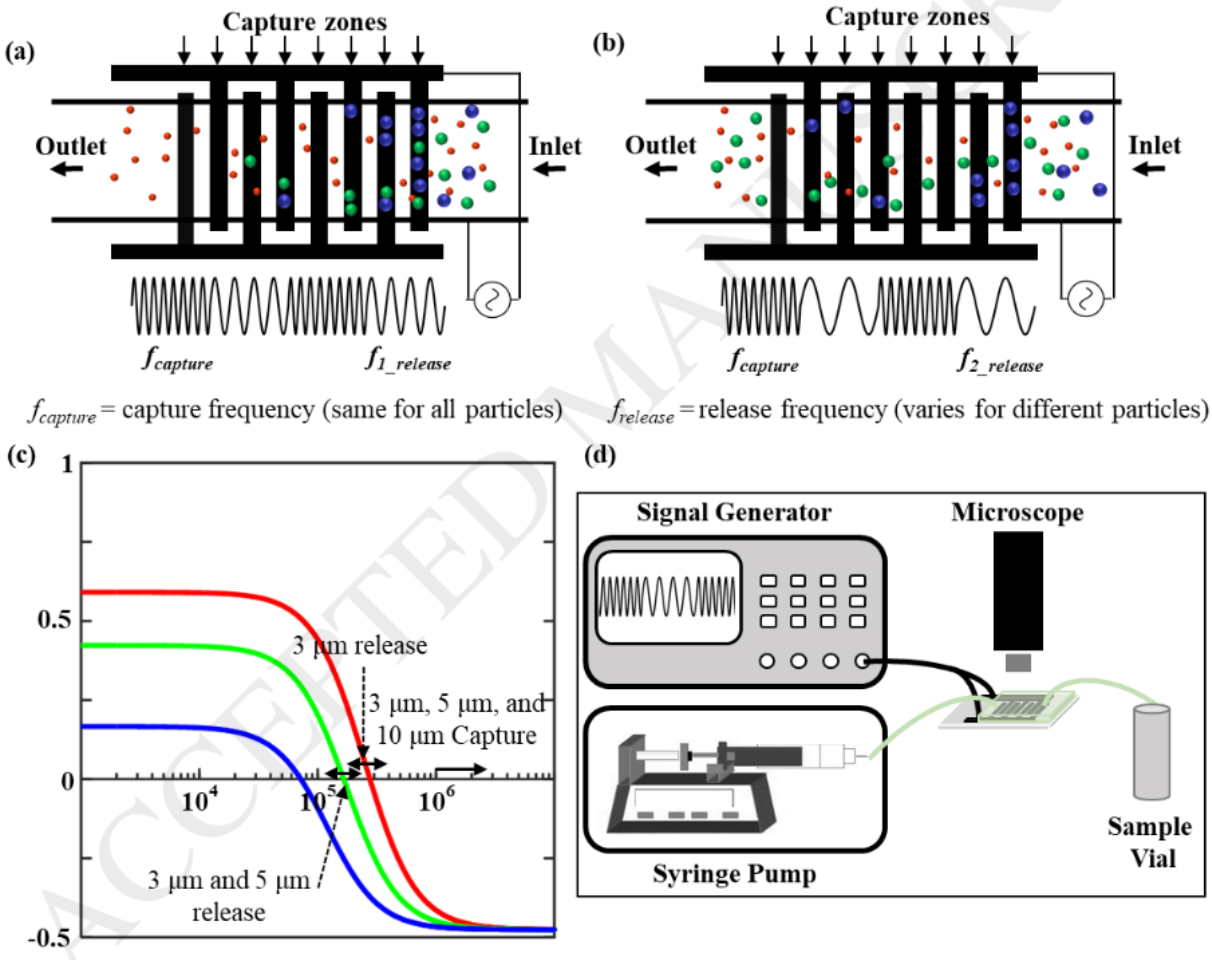

Figure 2: a) 2-D cross section simulation of electric field intensity square (E^2) for a 20 V_{pp} signal. E^2 versus location along x-axis indicating field capture zones, b) under nDEP (corresponding to cut-line at 2.5 µm below the top), and c) under pDEP (corresponding to cut-line at 2.5 µm above the device floor). d) Experimental flow rate vs. threshold frequency for polystyrene particles.

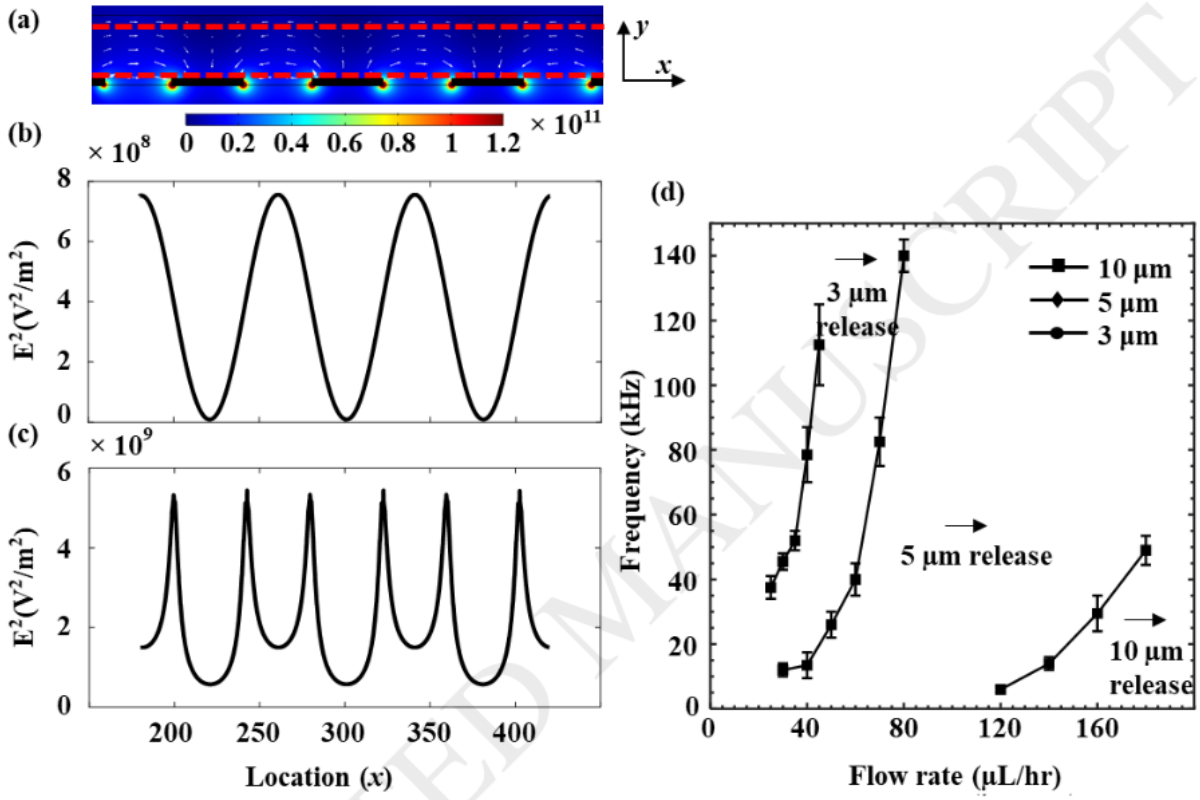

Figure 3: Time-lapse images showing (a, b, c) free-flowing 3 μm microspheres (circled red) with 5 μm and 10 μm microspheres being trapped. The 5 μm and 10 μm microspheres are entirely above gold electrodes and are not visible in these images. (Signal and flow parameters: $f_{capture}$ = 1 MHz, $f_{release}$ = 85 kHz, f_{shift} = 1 Hz, V_{pp} = 20 V, V_{flow} = 40 μL/hr). (d, e, f) free-flowing 3 μm and 5 μm microspheres (green circles) while 10 μm microspheres are retained. (Signal and flow parameters: $f_{capture}$ = 1 MHz, $f_{release}$ = 20 kHz, f_{shift} = 1 Hz, V_{pp}=20, V_{flow} = 40 μL/hr). The scale bar is 20 μm.

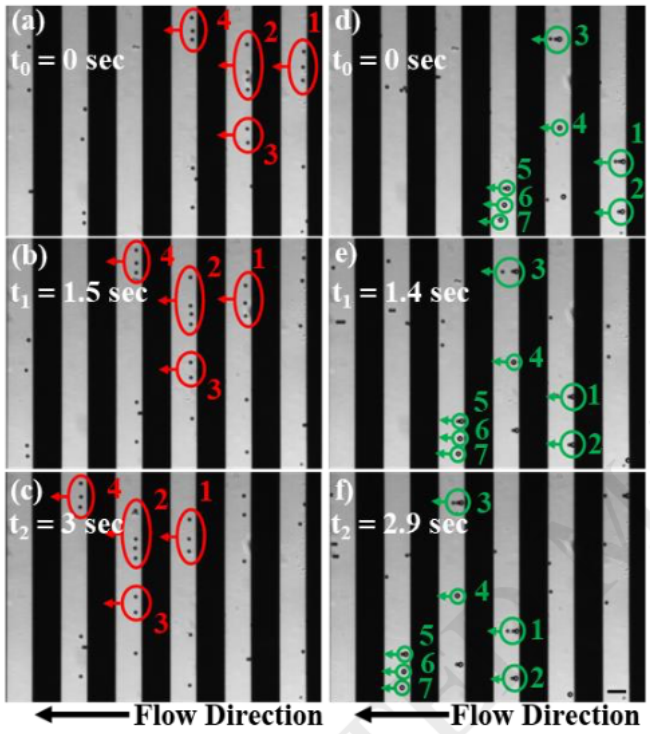

Figure 4: Quantitative analysis of collected samples. Dot plots of flow cytometry and the percentages of microspheres showing the sample composition a, d) before voltage application, b, e) after applying voltage and eluting 3 µm microspheres, and c, f) after applying voltage and eluting 3 µm and 5 µm microspheres. (n=3)

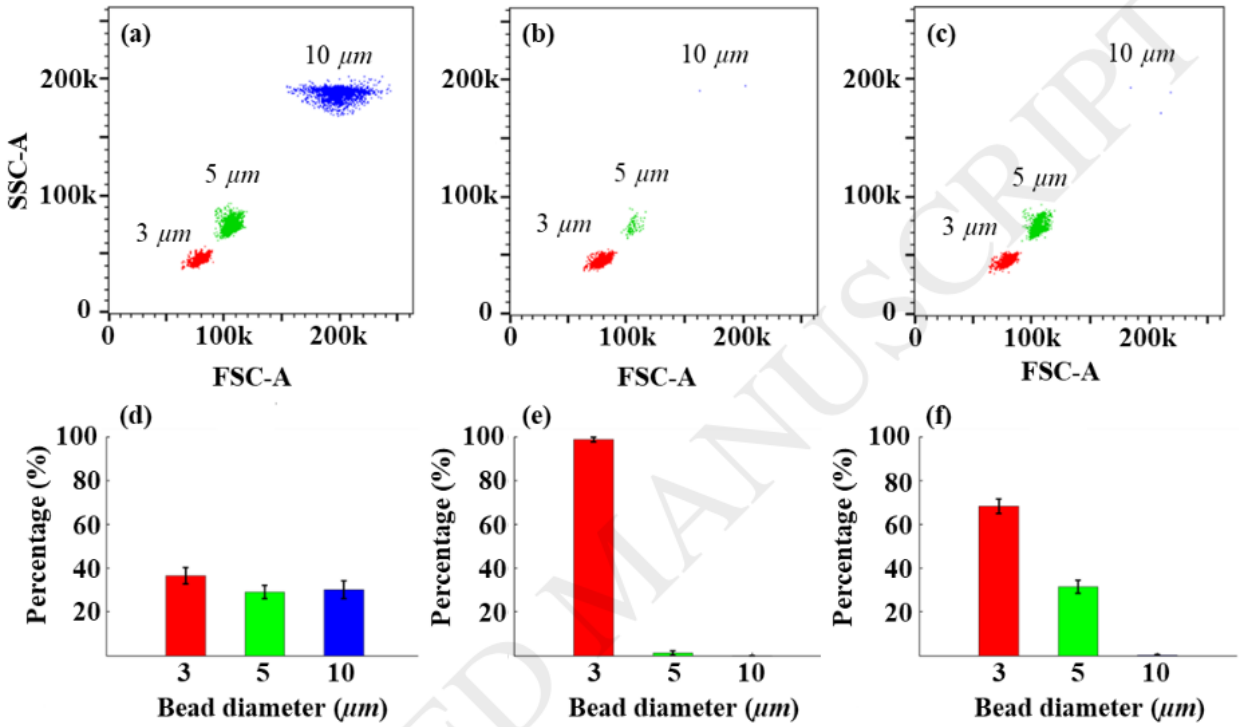

Figure 5: a) Real part of Clausius-Mossotti factor versus frequency for RBC and MCF7 cells. b) Enrichment efficiency of MCF7 cells vs. different voltage amplitudes (n=3). c) Light microscopy image of captured MCF7. d) Phase-contrast image of captured MCF7 cells at electrode edges with blood cells flowing down the channel. The scale bar is 20 µm.

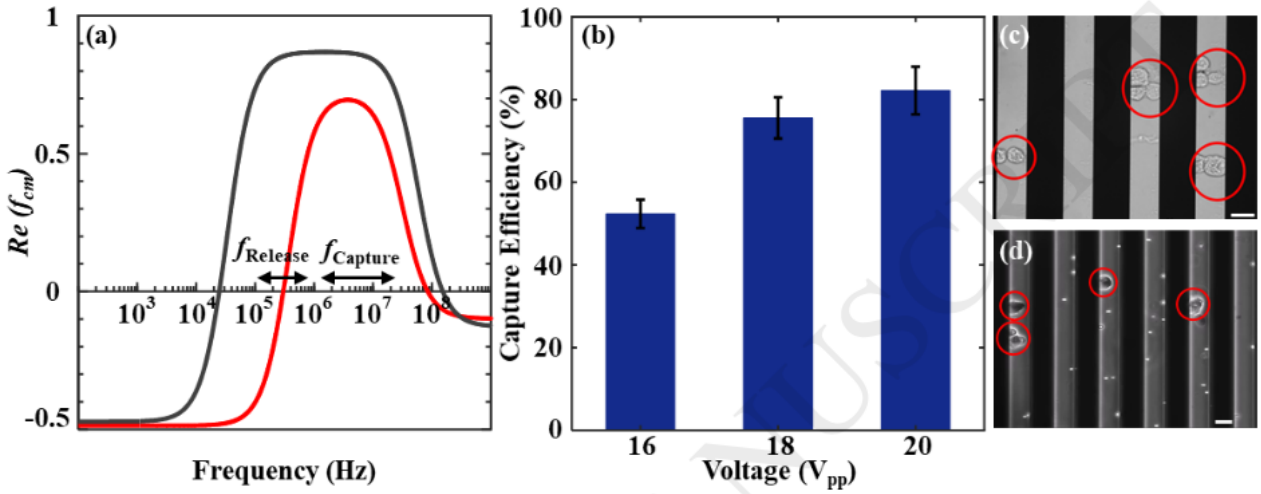

16